Published in final edited form as:
*J AAPOS*. 2006 April ; 10(2): 135–142.

# High-Resolution Magnetic Resonance Imaging Demonstrates Abnormalities of Motor Nerves and Extraocular Muscles in Patients With Neuropathic Strabismus

**Joseph L. Demer, MD, PhD**[a,b,c,d], **Maria Carolina Ortube, MD**[a], **Elizabeth C. Engle, MD**[e,f], and **Neepa Thacker, MD**[a]

a *Department of Ophthalmology, Jules Stein Dye Institute, University of California, Los Angeles, California*

b *Department of Neurology, University of California, Los Angeles, California*

c *Bioengineering Interdepartmental Program, University of California, Los Angeles, California*

d *Neuroscience Interdepartmental Program, University of California, Los Angeles, California*

e *Departments of Medicine (Genetics and Genomics) and Neurology, Children's Hospital Boston, Boston, Massachusetts*

f *Harvard Medical School, Boston, Massachusetts*

## Abstract

**Introduction—** Although the ocular motility examination has been used traditionally in the diagnosis of strabismus that is a result of cranial nerve (CN) abnormalities, magnetic resonance imaging (MRI) now permits the direct imaging of lesions in CN palsies.

**Methods—** Prospectively, nerves to extraocular muscles (EOMs) were imaged with T1 weighting in orbits of 83 orthotropic volunteers and 96 strabismic patients in quasicoronal planes using surface coils. Intraorbital resolution was 234–312 microns within 1.5- to 2.0-mm thick planes. CNs were imaged at the brainstem using head coils and T2 weighting, yielding 195 micron resolution in planes 1.0-mm thick in 6 normal volunteers and 22 patients who had oculomotor (CN3), trochlear (CN4), or abducens (CN6) palsies and Duane syndrome.

**Results—** Oculomotor (CN3) and abducens (CN6) but not trochlear (CN4) nerves were demonstrable in the orbit and skull base in all normal subjects. Patients with congenital CN3 palsies had hypoplastic CN3s both in orbit and skull base, with hypoplasia of involved EOMs. Patients with chronic CN6 and CN4 palsies exhibited atrophy of involved EOMs. Patients with Duane syndrome exhibited absence or hypoplasia of CN6 in both orbit and brainstem regions, often with mild hypoplasia and apparent misdirection of CN3 to the lateral rectus muscle. Unlike CN6 palsy, patients with Duane syndrome exhibited no EOM hypoplasia. Patients with congenital fibrosis exhibited severe hypoplasia of CN3, moderate hypoplasia of CN6, and EOM hypoplasia, particularly severe for the superior rectus and levator muscles.

**Conclusion—** High-resolution MRI can directly demonstrate pathology of CN3 and CN6 and affected EOM atrophy in strabismus caused by CN palsies. Direct imaging of CNs and EOMs by MRI is feasible and useful in differential diagnosis of complex strabismus.

Reprint Requests: Joseph L. Demer MD, PhD, Jules Stein Eye Institute, 100 Stein Plaza UCLA, Los Angeles CA 90095-7002 (e-mail: jld@ucla.edu)..

Presented at the AAPOS Meeting Orlando Florida March, 2005.

Supported by grants from the National Eye Institute: EY08313, EY13583, and EY00331. Also supported by an unrestricted grant from Research to Prevent Blindness. Joseph L. Demer is the Leonard Apt Professor of Ophthalmology.

Since the discovery of x-rays, imaging has become pervasive in modern medicine. In the evaluation of neuropathic strabismus, the head frequently is imaged by computed x-ray tomography (CT) or magnetic resonance imaging (MRI) to rule out large structural lesions, such as infarcts, tumors, or aneurysms. Nevertheless, evidence for the existence of cranial nerve (CN) palsies or pareses has, up to this time, been indirect, entirely based on clinical findings such as ocular motility and alignment patterns. With only rare exceptions, it has been impossible to directly confirm by imaging the existence of motor CN pathology in presumably neuropathic strabismus.

Technical improvements in MRI now afford the opportunity for detailed study of the functional anatomy of extraocular muscles (EOMs) and CNs in the orbits of living subjects,[1] and CNs can be imaged against the surrounding cerebrospinal fluid as they exit the brainstem.[2] This prospective study was conducted to examine the utility of imaging for direct confirmation of lesions in presumed neuropathic strabismus.

## SUBJECTS AND METHODS

In a prospective study of imaging ongoing since 1990, a total of 83 orthotropic volunteers and 96 patients with strabismus presumed on clinical grounds to be caused by cranial neuropathy underwent high-resolution orbital MRI under a prospective protocol. Orthotropic volunteers were recruited by advertising; the patients were recruited from referral strabismus practices and a collaborative study of EOM dysinnervation disorders. In all subjects, written informed consent was obtained prospectively according to a protocol approved by relevant institutional review boards for the protection of human subjects. All subjects underwent complete ophthalmologic examination, with particular attention to ocular motility. In addition to measurement of alignment using prism-cover testing and photography in 9 diagnostic gaze positions, all appropriate strabismic patients underwent Hess screen testing.

Imaging was performed using a 1.5-T General Electric Signa scanner (Milwaukee, WI). Orbital imaging was performed using an array of surface coils embedded in a transparent facemask (Medical Advances, Milwaukee, WI) and using fixation targets to avoid eye motion artifacts.[3,4] The head was stabilized in the supine position by tightly fastening the surface coil mask to the face using headbands and by fixing the mask to the scanner gantry using foam cushions and tape. These measures avoided head rotation during scanning. An adjustable array of illuminated fixation targets was secured in front of each orbit, with the center target in subjective central position for each eye and, in selected cases, in secondary and tertiary gaze positions. Imaging at and posterior to the orbital apex in some subjects was performed using the standard head coil. When surface coils were used, images of 2-mm thickness in a matrix of 256 × 256 were obtained over a field of view of 6 to 8 cm for a resolution in plane of 234 to 312 $\mu$m, respectively. Axial scout images were obtained, as well as quasicoronal images perpendicular to the long axis of the orbit, and quasisagittal images parallel to the long axis of the orbit.

In 6 normal volunteers and 22 strabismic patients, imaging of the CNs at the brainstem was performed in 1-mm thickness image planes using the heavily T2-weighted FIESTA sequence, which provides good contrast of the cranial nerves against the surrounding cerebrospinal fluid.[2] In-plane resolution was 195 $\mu$m over a 10-cm field of view (matrix 512 × 512) with 10 excitations.

Digital MRI images were transferred to Macintosh® computers (Apple Computer, Inc. Cupertino, CA), converted into 8-bit tagged image file format (TIFF), and examined using the program *NIH Image* (W. Rasband, National Institutes of Health; available by ftp from zippy. nimh.nih.gov or on floppy disk from NTIS, 5285 Port Royal Road, Springfield, VA 22161,

part number PB95-500195GEI). Cranial nerve sizes were not quantified in the current project, although with a larger sample size, it may become possible to do so for the proximal CN3, and possibly for CN6, when optimal imaging is obtained. Motor nerves in the anterior orbit are too small for quantitative measurements in the available images. Reported abnormalities were evident here from visual inspection and comparison with control images.

## RESULTS

### Normal Subjects

**Extraocular Muscle Imaging—**The stereotypic locations and sizes of normal EOMs have been reported using this technique.[1,4–12] All findings were consistent with previous reports.

**Imaging of Intraorbital Motor Nerves—**It was possible to examine, in the deep orbit, the motor nerves to the EOMs in image planes of 1.5- to 2-mm thickness and field of view 6 to 8 cm. In normal subjects, all of the motor nerves to the EOMs could be visualized in some cases (Fig. 1). Motor nerves to the medial rectus (MR), inferior rectus (IR), inferior oblique (IO), and lateral rectus (LR) muscles were consistently demonstrable, although the trochlear nerve (CN4) could only occasionally be demonstrated. The superior division of the oculomotor nerve (CN3) is small and can only occasionally be traced in normal subjects to the inferior surface of the superior rectus (SR), where it runs anteriorly before entry. The inferior division of CN3 can be traced from the cavernous sinus, where CN3 divides into superior and inferior divisions. This bifurcation cannot be resolved by this MRI technique in normal subjects. The much-larger inferior division forms a readily visualized manifold as it courses anteriorly to send out a nasal branch to the MR and an inferior branch that in turn bifurcates to innervate the IR and, more anteriorly, the inferior oblique (IO) via the neurofibrovascular bundle.[13] The nerve entry to the IO is compact and surrounded by the dense connective tissue of the IO pulley. The intraorbital motor nerves from the inferior division of CN3 can readily be visualized and traced by MRI from the orbital apex to the target EOMs; even the epimuscular innervation of the normal LR, MR, and IR can be visualized. For these, motor nerves typically divide to form arborizations that course anteriorly along the orbital surface of the EOMs before entering them. This is evident for the IR in the top center panel of Fig. 1. The CN4 is small and enters the superior oblique muscle (SO) from a superolateral angle deep in the orbit; it usually was not visualized in normal subjects. The normal abducens nerve (CN6) is larger than CN4, coursing from the superior orbital apex to form an arborization along the orbital surface of the LR, where it enters to innervate the LR. MRI typically can visualize the normal CN6 and its epimuscular arborization, which is typically 4 mm more posterior than the entry of the branch of CN3 to the IR and 6 to 8 mm more posterior than the entry of the branch of CN3 to MR. By tracing nerve cross sections in multiple, adjacent MRI planes, it was in nearly all cases possible to differentiate CN6 from branches of CN3.

**Imaging of Normal Intracranial Motor Nerves—**In 6 normal subjects, heavily T2-weighted imaging of the skull base region was conducted in 60 contiguous 1-mm thickness slices at 390-$\mu$m resolution in the plane of the optic chiasm and major CNs that innervate the orbit. Examination of contiguous thin image planes avoided the possibility of missing small structures between planes and permitted confirmation of structures by their presence in contiguous planes. In all normal subjects, it was possible to resolve CN3 in multiple adjacent image planes (Fig. 2A). This technique has sufficient resolution to demonstrate the normal CN6 coursing anteriorly from the pons, usually in 2 or 3 contiguous image planes (Fig. 2B). In adjacent sections, CN6 could be traced from the pons across the cerebrospinal fluid space to the clivus in every normal subject. The CN4 could be imaged only occasionally (Fig. 2A).

## Patients With Neuropathic Strabismus

**Acquired Oculomotor Palsy—**The orbits were imaged in 14 patients with partial or complete CN3 palsy, of which 12 cases were acquired and 2 congenital. Findings in some of these cases have been reported elsewhere.[1] In general, EOMs innervated by CN3 exhibited marked and generalized atrophy when acquired lesions interrupted innervation, but EOM volume was preserved by aberrant innervation.

In one case of isolated, progressive acquired MR paralysis in a 5-year-old girl lead to marked right exotropia (Fig. 3). A mildly contrast-enhancing mass was identified in the apex of the right orbit on the CN3 branch to the MR (Fig. 4). This mass was compatible with an isolated neuroma of the motor nerve to the MR, distal to the division of the inferior branch of CN3 into branches innervating the IO and IR muscles.

In one case of slowly progressive, partial right CN3 palsy in an adult, repeated conventional head MRI failed to disclose a lesion. This imaging was in 5-mm thickness planes. The patient exhibited mild blepharoptosis, mydriasis, and limitation of adduction, supraduction, and infraduction. High-resolution orbital imaging disclosed atrophy of the MR, IR, SR, and levator muscles in the right orbit, along with reduction in size of the motor nerves to each of these EOMs (Fig. 5). A magnetic resonance angiogram was performed, which showed only normal cerebral vessels (Fig. 6). However, high-resolution MRI of the skull base in 1-mm thick planes demonstrated a contrast-enhancing fusiform lesion in the right CN3 that was consistent with a neuroma (Fig. 7).

**Congenital Oculomotor Palsy—**In the 2 congenital cases, EOM atrophy or hypoplasia also was evident, but affected the posterior more than the anterior EOM belly. This is evident in the patient illustrated in Fig. 8, in whom there was marked congenital limitation of adduction of the right eye and mild blepharoptosis. Motility of the left eye appeared clinically normal. Figure 8 illustrates hypoplasia and abnormal bright signal in the deep portion of the right MR and IR muscles, along with reduced size of all branches of the inferior division of CN3 in the right orbit. Although present in the clinically unaffected left orbit, the branches of the left CN3 also were small. Imaging of CN3 at the brainstem yielded an unanticipated finding in this case (Fig. 9). The right CN3 appeared absent, and the left CN3 was barely large enough to image. On the basis of residual clinical function, vestiges of both CN3s must have been present, yet they were severely and asymmetrically hypoplastic. The second patient had congenital right exotropia and hypotropia with absent levator muscle function. Imaging was performed in the orbits only and showed profound hypoplasia of the IR muscle.

**Congenital Fibrosis of the Extraocular Muscles (CFEOM)—**Imaging was performed in 18 dominant and 4 sporadic cases of CFEOM. Findings were consistent with earlier reports from this ongoing study. CFEOM1, caused by a mutation in the developmental kinesin KIF21A, consistently was associated with severe hypoplasia of the SR and levator muscles, hypoplasia of all of the motor nerves in the orbit, and misdirection of CN3.[14] Intimate continuity between the inferior division of CN3 and the LR muscle was observed in 5 cases, which was suggestive of aberrant innervation of LR by CN3. Contractile thickening of the LR on infraduction, associated with A-pattern exotropia, provided functional evidence suggesting that the LR was innervated by a motor nerve that normally is destined for the IR muscle. In 4 orbits of 3 subjects, the same motor nerve, probably CN6, entered and apparently innervated both the LR and IR muscles. Most severely hypoplastic was CN3, particularly as imaged at the brainstem. Nearly every EOM exhibited structural abnormality or abnormal bright internal signal on T1 imaging.

**Trochlear Palsy—**A total of 55 patients with CN4 palsies underwent orbital imaging. All exhibited atrophy or absence of the involved SO muscle. Findings were similar in acquired and congenital cases. These results are consistent with previous reports on patients accumulated in the early years of this study.[1,9,11,15] The CN4 was not systematically investigated at the brainstem or in the orbit because MRI cannot consistently demonstrate CN4 even in normal subjects.

**Acquired Abducens Palsy—**The orbits were imaged in 13 patients with acquired CN6 palsy, and general findings were consistent with previous descriptions.[1] In all cases, the affected LR muscle was markedly atrophic.

The CN6 was imaged at the brainstem in a 75-year-old man with progressive bilateral CN6 paresis caused by a clivus chordoma of 2 years' duration that was treated with radiotherapy. Initial presentation showed that the CN6 paresis was more severe on the left side. In both orbits, coronal T1-weighted MRI demonstrated small CN6s. At the brainstem, T2-weighted MRI demonstrated striking atrophy of both CN6s, which was most severe for the left CN6 that have been first involved clinically (Fig. 10).

**Duane Syndrome—**The orbits were imaged in 13 patients with unilateral or bilateral Duane retraction syndrome. All of these patients exhibited globe retraction and palpebral fissure narrowing in adduction, as well as limitation of abduction and/or adduction. Cases were included of primarily limited abduction, primarily limited adduction, and limitation of both abduction and adduction. Irrespective of the preservation of abduction range, the LR exhibited a normal size in all but one case. That patient, reported elsewhere, had both Duane syndrome and a large skull base meningioma directly compressing multiple CNs.[16]

In recently imaged patients with Duane syndrome, CN6 in the affected orbit was small or absent and CN3 was in continuity with it, which is suggestive of aberrant innervation of LR by CN3. This is illustrated by the case of a 15-year-old girl with sporadic unilateral type 1 Duane syndrome on the right side. As illustrated in Fig. 11, the right LR muscle bulk was normal. However, the right CN6 could not be identified using high-resolution quasi-coronal MRI of the orbit, and the right CN3 could be traced to the border of the LR and apparently entered to innervate it. Oblique axial T2-weighted imaging of the brainstem in this same patient demonstrated the absence of the right CN6 but a normal CN6 on the clinically unaffected left side (Fig. 12).

The finding of CN6 abnormality in Duane syndrome has been correlated reliably with Duane syndrome in the clinically affected orbit. Occasionally, CN6 has been found to be hypoplastic in the clinically unaffected orbit of apparently unilateral cases, suggesting subclinical bilateral involvement. Although in some cases of Duane syndrome a small CN6 could occasionally be identified entering the affected LR, CN3 appeared to coinnervate LR as well.

## DISCUSSION

Orbital imaging, particularly using MRI, has broadened understanding of the anatomy and physiology of the EOMs and their associated connective tissues.[5,17] In living humans, it is now possible to image at near microscopic resolution the physiologic changes associated with conjugate eye movements, vergence, and accommodation.[6] It has been possible for some years to use clinically available equipment to image the size, contractility, and position of each EOM.

The current study was a directed, prospective effort to understand the effects of CN abnormalities on the functional anatomy of the EOMs and to image these CNs directly. This required recruitment of patients and acquisition of data over the course of a long time period.

Naturally, technical progress during this decade resulted in continuously improving capabilities. The earliest imaging in this series probably missed some abnormalities that were detectable later using improved technique. Further imaging studies are likely to disclose currently unforeseen pathologic mechanisms.

This study is a cumulative compilation of an extensive data set that also has been the subject of interim reports focused on narrower, and often quantitative, questions. The current study is not quantitatively informative concerning the prevalence of pathologic findings but rather proof of the concept that modern MRI can directly demonstrate CN pathology in situations in which this pathology causes strabismus. The abnormalities reported here were obvious from direct inspection of the MRI images and did not require sophisticated quantitative morphometry. On the basis of the sheer number of significant imaging findings reported here, particularly clinically unsuspected ones, it can be concluded that EOM and nerve imaging can provide important information in patients with strabismus. In many cases, these findings supported definitive management decisions.

In some clinically unilateral cases of CN palsy, MRI suggested bilateral-but-asymmetrical involvement more severe on the clinically apparent side. Perhaps such unsuspected bilateral involvement is because normal motor nerves to the EOMs may have a generous safety margin of axons in excess of the minimal number required to support full ductions. It is also likely that clinical diagnosis of version deficits is less sensitive when both orbits harbor abnormalities compensated by central innervational effort. At any rate, the current findings indicate that clinically normal versions do not rule out subtle CN abnormalities involving innervation to EOMs.

Today, most orthopedic, general, and certainly neurosurgeons commonly obtain imaging studies before operating on a patient. For example, a PubMed search of preoperative imaging returned 785 reports since 1971 representing a broad range of surgical specialties, including general surgery, neurosurgery, cardiac surgery, orthopedics, otolaryngology, oral surgery, and gynecology (J. Demer, personal observation, PubMed, July 29, 2005). Supporting an earlier report,[1] current findings suggest that strabismus surgeons expand their use of preoperative imaging. Ophthalmologists must educate radiologists in the interpretation of high-resolution EOM images because these colleagues typically are unfamiliar with detailed orbital anatomy and EOM pathophysiology. Strabismologists should examine the images because most diagnosis can be made during inspection by an ophthalmologist familiar with the clinical situation.

## References

1. Demer JL. A 12 year, prospective study of extraocular muscle imaging in complex strabismus. J AAPOS 2003;6:337–47. [PubMed: 12506273]
2. Seitz J, Held P, Strotzer M, et al. MR imaging of cranial nerve lesions using six different high-resolution T1 and T2(*)-weighted 3D and 2D sequences. Acta Radiol 2002;43:349–53. [PubMed: 12225473]
3. Demer, JL.; Miller, JM. Orbital imaging in strabismus surgery. In: Rosenbaum, AL.; Santiago, AP., editors. Clinical strabismus management: principles and techniques. Philadelphia: WB Saunders; 1999. p. 84-98.
4. Clark RA, Miller JM, Demer JL. Three-dimensional location of human rectus pulleys by path inflections in secondary gaze positions. Invest Ophthalmol Vis Sci 2000;41:3787–97. [PubMed: 11053278]
5. Demer, JL. Anatomy of strabismus. In: Taylor, D.; Hoyt, C., editors. Pediatric ophthalmology and strabismus. 3. London: Elsevier; 2005. p. 849-61.
6. Demer JL, Kono R, Wright W. Magnetic resonance imaging of human extraocular muscles in convergence. J Neurophysiol 2003;89:2072–85. [PubMed: 12686579]

7. Demer JL, Oh SY, Clark RA, Poukens V. Evidence for a pulley of the inferior oblique muscle. Invest Ophthalmol Vis Sci 2003;44:3856–65. [PubMed: 12939301]
8. Demer JL, Oh SY, Poukens V. Evidence for active control of rectus extraocular muscle pulleys. Invest Ophthalmol Vis Sci 2000;41:1280–90. [PubMed: 10798641]
9. Demer JL, Miller JM. Magnetic resonance imaging of the functional anatomy of the superior oblique muscle. Invest Ophthalmol Vis Sci 1995;36:906–13. [PubMed: 7706039]
10. Demer JL, Kerman BM. Comparison of standardized echography with magnetic resonance imaging to measure extraocular muscle size. Am J Ophthalmol 1994;118:351–61. [PubMed: 8085593]
11. Kono R, Demer JL. Magnetic resonance imaging of the functional anatomy of the inferior oblique muscle in superior oblique palsy. Ophthalmology 2003;110:1219–29. [PubMed: 12799250]
12. Kono R, Clark RA, Demer JL. Active pulleys: Magnetic resonance imaging of rectus muscle paths in tertiary gazes. Invest Ophthalmol Vis Sci 2002;43:2179–88. [PubMed: 12091414]
13. Stager DR. The neurofibrovascular bundle of the inferior oblique muscle as its ancillary origin. Trans Am Ophthalmol Soc 1996;94:1073–94. [PubMed: 8981719]
14. Demer JL, Clark RA, Engle EC. Magnetic resonance imaging evidence for widespread orbital dysinnervation in congenital fibrosis of extraocular muscles due to mutations in KIF21A. Invest Ophthalmol Vis Sci 2005;46:530–9. [PubMed: 15671279]
15. Demer, JL.; Miller, MJ.; Koo, EY.; Rosenbaum, AL.; Bateman, JB. True versus masquerading superior oblique palsies: Muscle mechanisms revealed by magnetic resonance imaging. In: Lennerstrand, G., editor. Update on strabismus and pediatric ophthalmology. Boca Raton (FL): CRC Press; 1995. p. 303-6.
16. Silverberg M, Demer JL. Duane's syndrome with compressive denervation of the lateral rectus muscle. Am J Ophthalmol 2001;131:146–8. [PubMed: 11162999]
17. Demer JL. Pivotal role of orbital connective tissues in binocular alignment and strabismus. The Friedenwald lecture. Invest Ophthalmol Vis Sci 2004;45:729–38. [PubMed: 14985282]

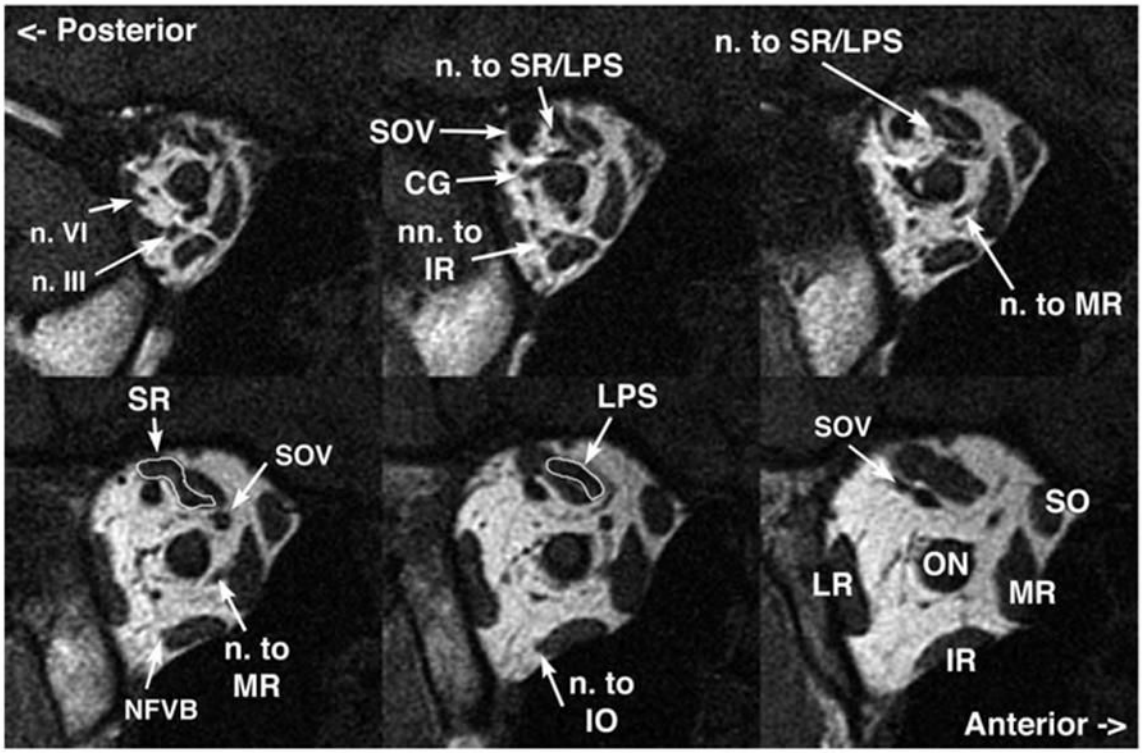


**FIG 1.**

Coronal MRI of deep right orbit of normal subject in central gaze demonstrating details of innervation in 2-mm thickness planes. CG: ciliary ganglion; IO: inferior oblique muscle (m); IR: inferior rectus (m); LPS: levator palpebrae superioris (m); LR: lateral rectus (m); M's: Mueller's (m); MR: medial rectus (m); ON: optic nerve (n); PPG: pterygopalatine ganglion; SO: superior oblique (m); SOV: superior orbital vein (v); SR: superior rectus (m). m, muscle; v, vein.

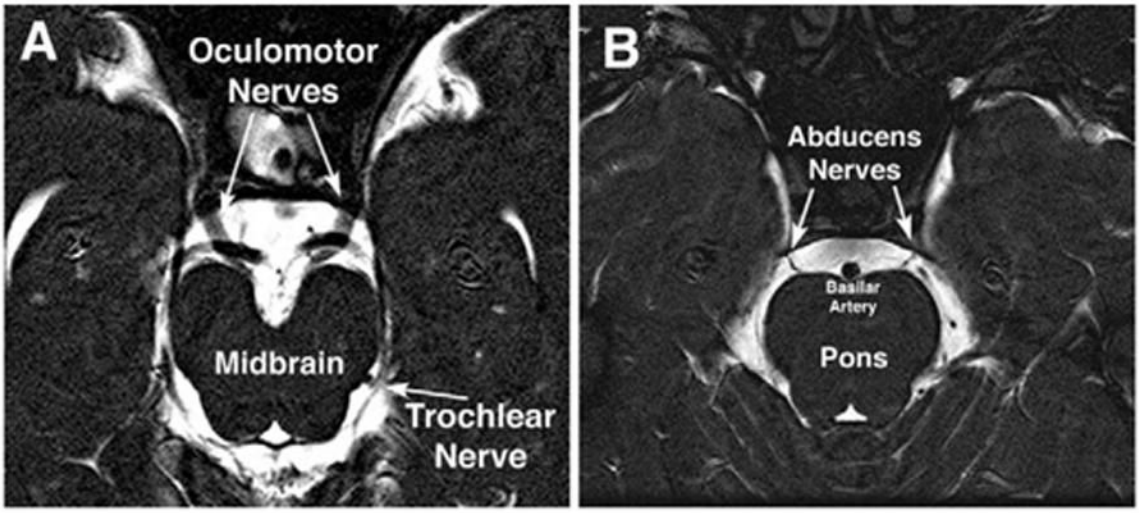


**FIG 2.**

Oblique, axial heavily T2-weighted MRI images of 1-mm thickness from a normal subject. A, Normal course of the large oculomotor and barely resolvable trochlear nerves from the midbrain highlighted against the bright signal of the surrounding cerebrospinal fluid. B, Normal course of the abducens nerves from the pons highlighted against the bright signal of the surrounding cerebrospinal fluid.

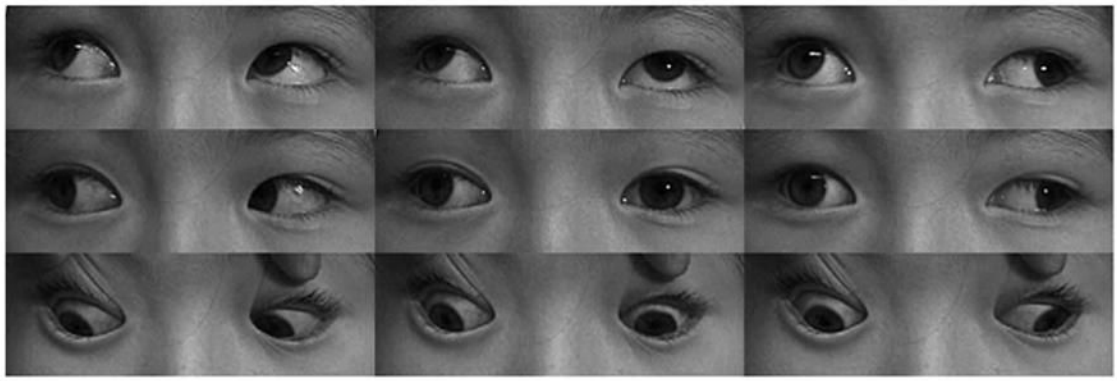

**FIG 3.**
Clinical versions showed marked limitation of adduction of the right eye of child with acquired right medial rectus paralysis caused by motor nerve neuroma.

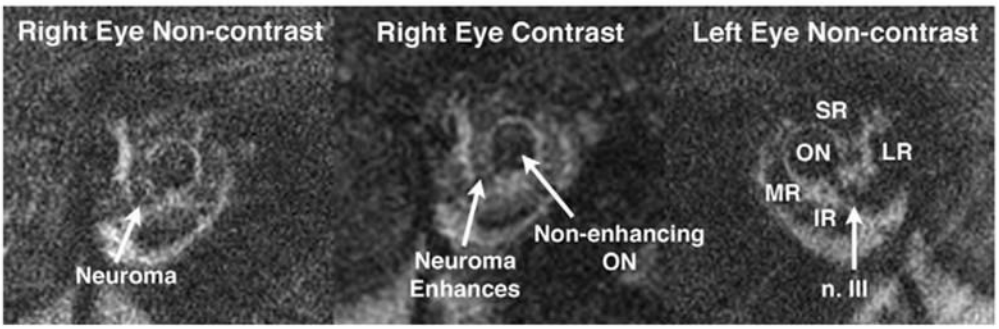


**FIG 4.**

Coronal MRI of case illustrated in Fig. 3 shows a fusiform enlargement between the right lateral rectus (LR) and optic nerve (ON) in the region of the motor nerve to the medial rectus (MR) muscle. Like the extraocular muscles, but unlike the optic nerve, this enlargement enhanced mildly with gadodiamide contrast, confirming a neuroma. A normal-sized oculomotor (n. III) was present on the uninvolved left side. IR: inferior rectus muscle; SR: superior rectus muscle.

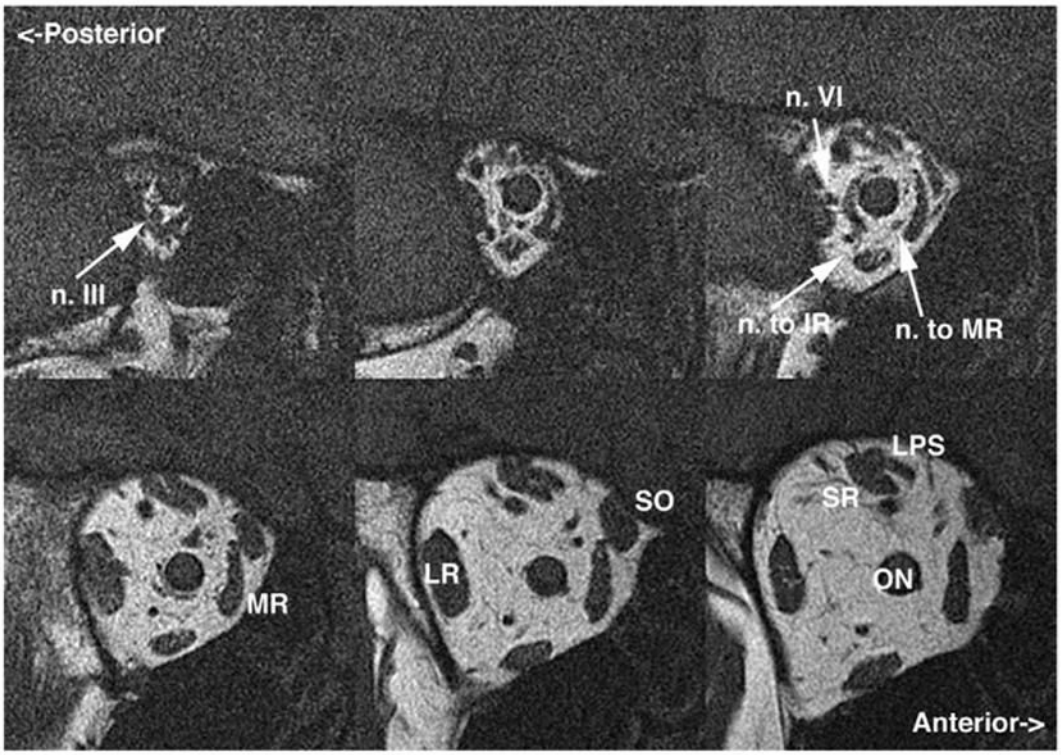


**FIG 5.**

Coronal plane MRI of the right orbit of an adult with progressive acquired right oculomotor palsy showing atrophy of the IR, medial rectus (MR), superior rectus (SR), and levator muscles, along with motor nerves to each. Note the normal caliber of the abducens nerve (n. VI) and bulk of the lateral rectus (LR) muscle for comparison. LPS: levator palpebrae superioris muscle; ON: optic nerve. Image planes are 2-mm thick.

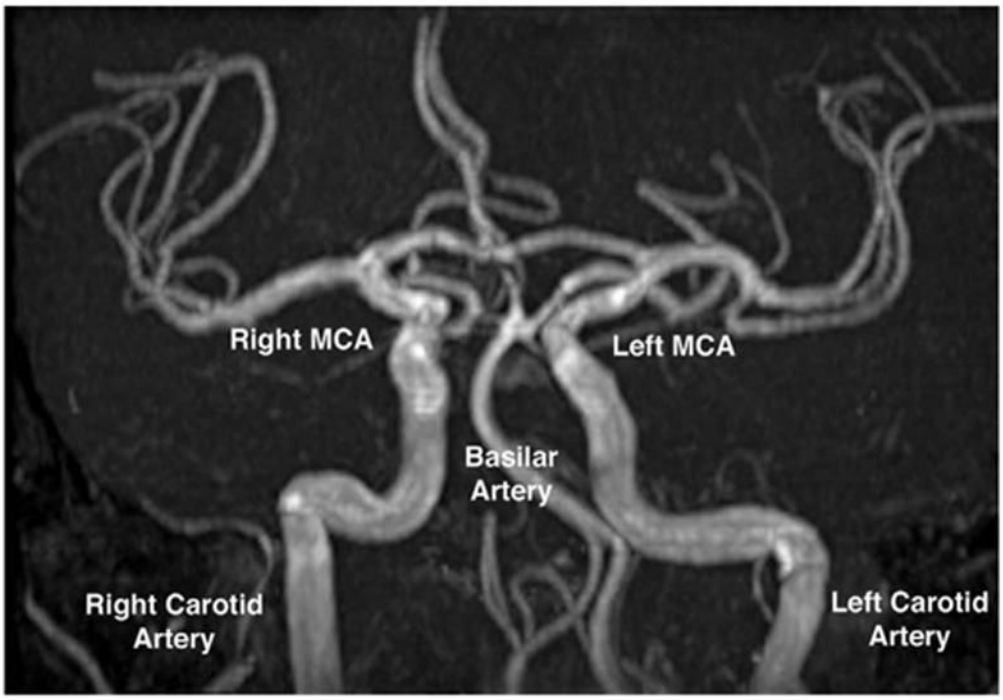


**FIG 6.**
Magnetic resonance angiography shows normal arteries in the region of the circle of Willis in the patient of Fig. 5, who had progressive right oculomotor palsy. MCA: middle cerebral artery.

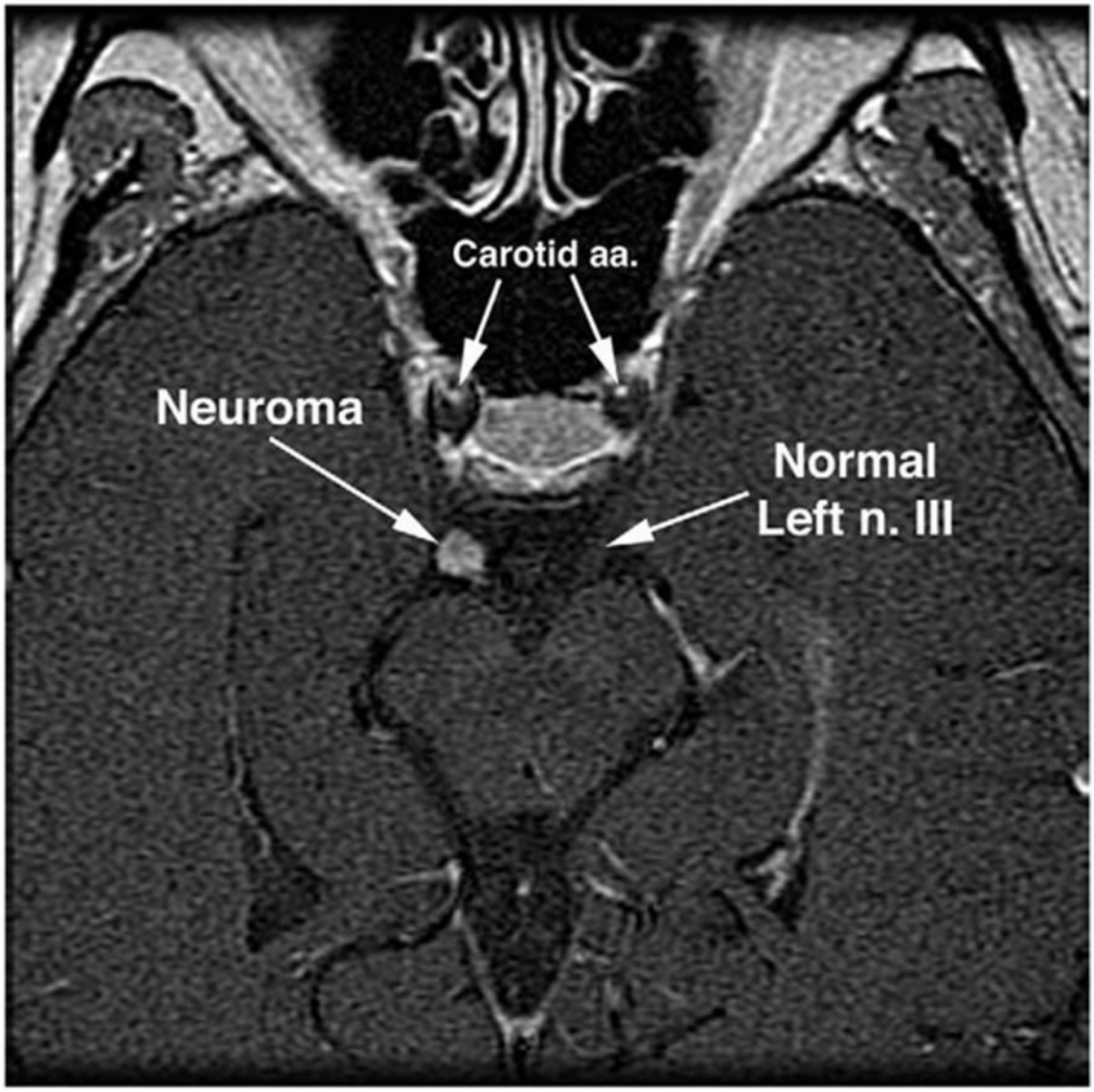


**FIG 7.**
Gadolinium contrast-enhanced, axial MRI of midbrain and oculomotor nerves of patient in Fig. 5 with progressive right oculomotor palsy. Note spherical mass on the right oculomotor nerve (n. III) consistent with a neuroma.

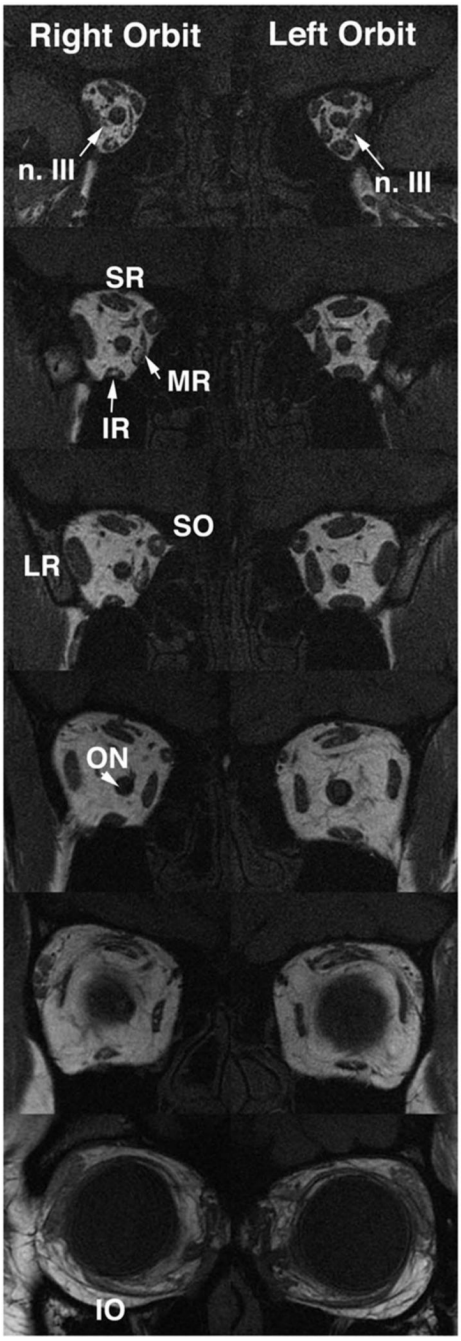


**FIG 8.**

Coronal MRI of both orbits of child with partial congenital right oculomotor palsy. Note hypoplasia and abnormal bright signal in deep portion of the right medial rectus (MR) and inferior rectus (IR) muscles, as well as reduced size of all branches of the oculomotor nerve in the right orbit. Branches of the left oculomotor nerve are also small. Entry of the abducens nerve into the lateral rectus muscle is more posterior to these image planes, and so is not confused with oculomotor nerve branches. The images are 2-mm thick. SR: superior rectus; SO: superior oblique; ON: optic nerve.

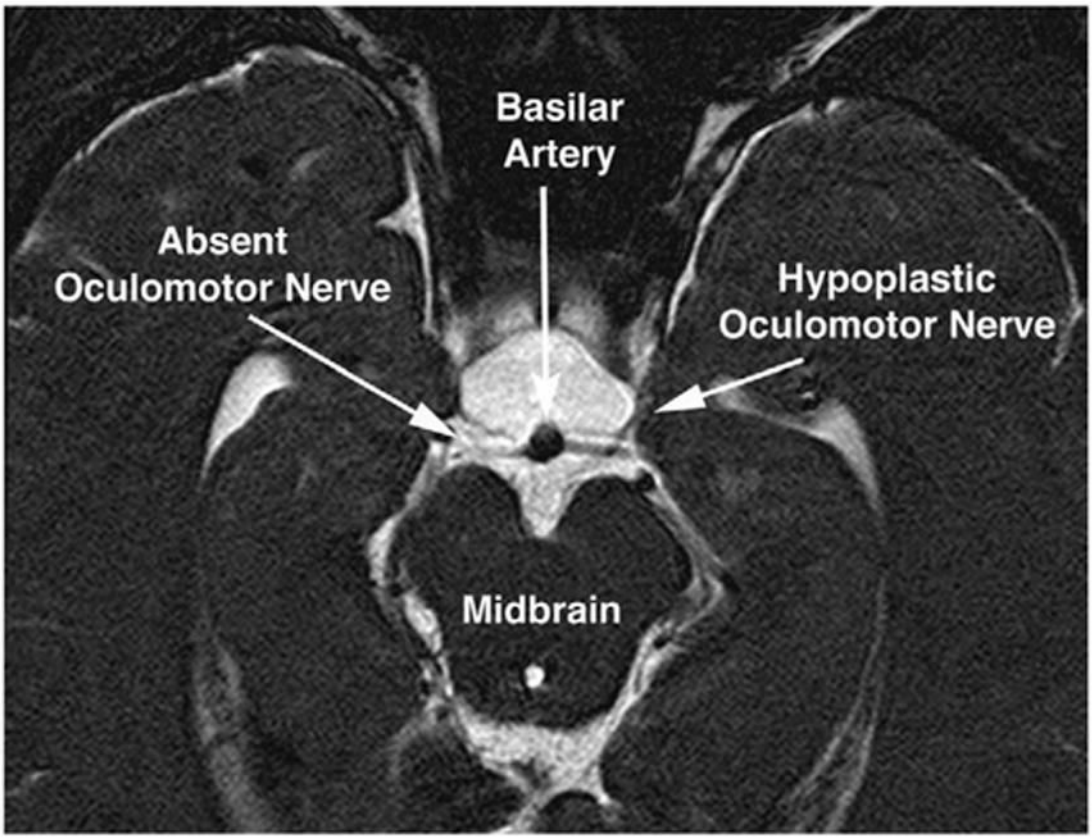


**FIG 9.**

Oblique axial T2-weighted MRI of the midbrain of the child in Fig. 8 with partial congenital right oculomotor palsy. Note apparent absence of the right oculomotor nerve, and marked hypoplasia of the left oculomotor nerve. Thus, the anatomic findings of bilateral oculomotor hypoplasia were more severe than the clinical findings of partial right unilateral oculomotor palsy. The images are 1-mm thick.

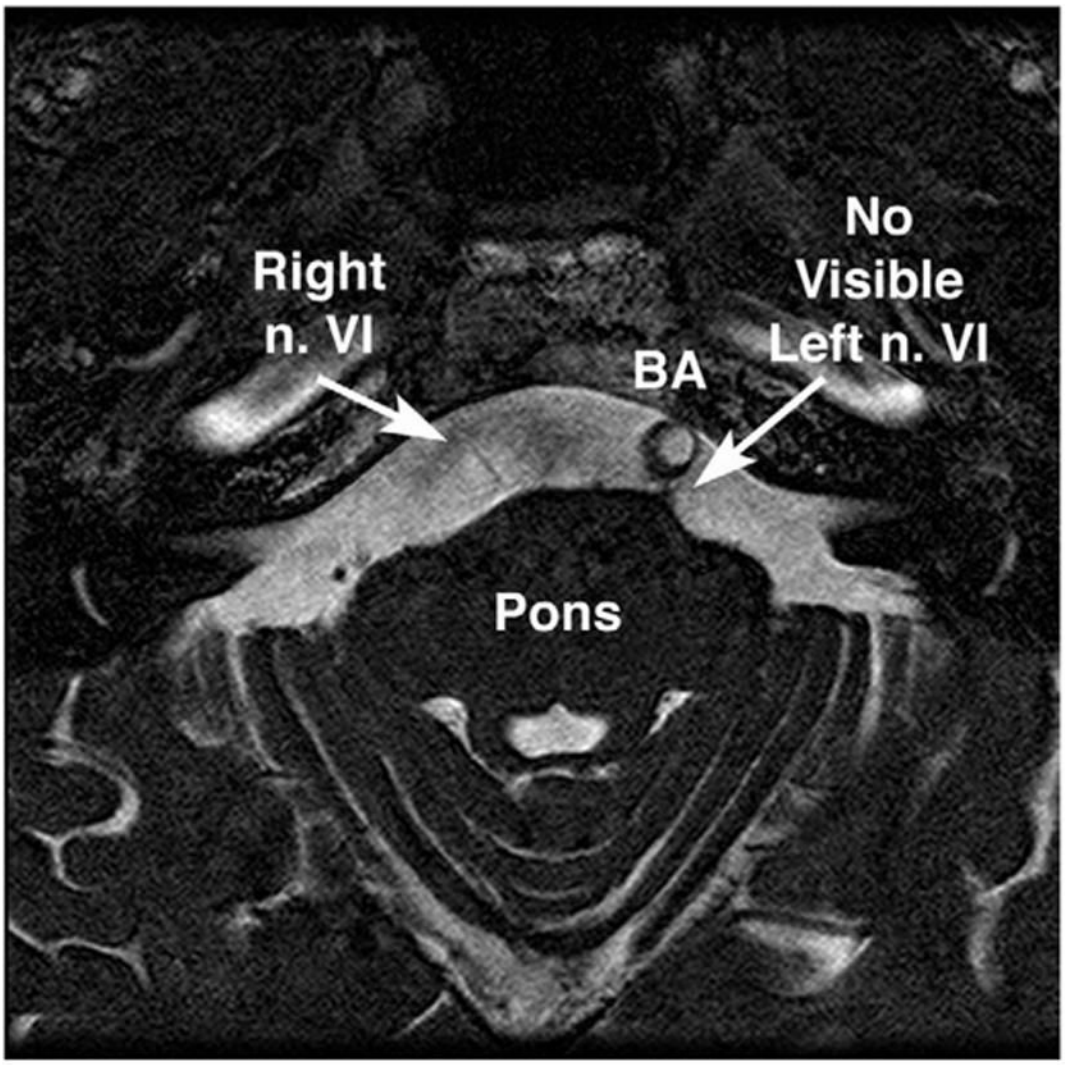


**FIG 10.**

Oblique axial T2-weighted MRI of the midbrain of a 75-year-old man with progressive bilateral abducens paresis caused by clivus chordoma. Note the marked atrophy of the right abducens nerve (n. VI), and absence of visible left n. VI. These findings were confirmed in contiguous image planes. The basilar artery (BA) is displaced to the left, a common normal variant. 1mm image plane thickness, in plane resolution 390 microns.

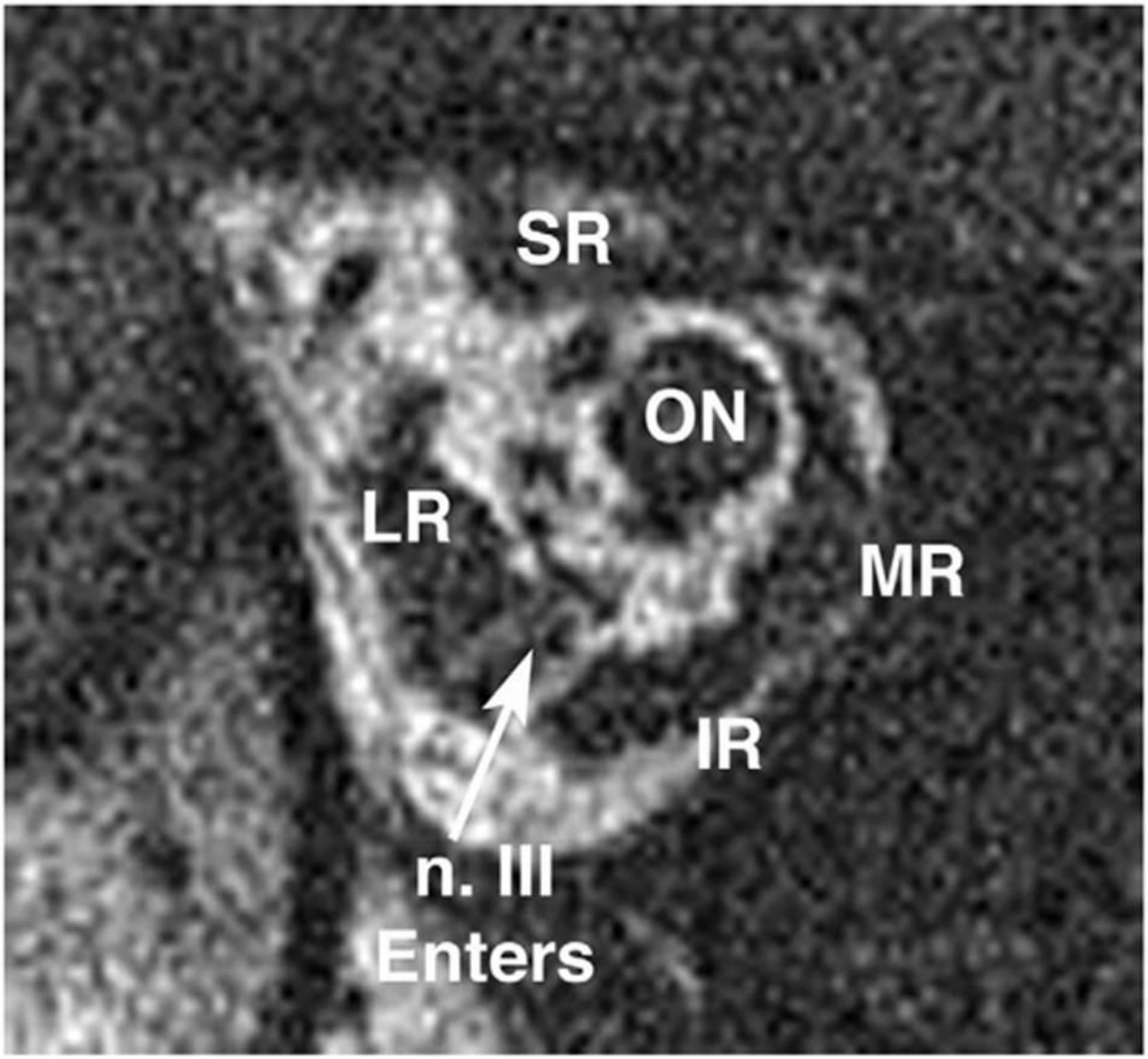


**FIG 11.**

Deep coronal MRI of the right orbit of a 15-year-old girl with right type 1 Duane syndrome. Note normal lateral rectus (LR) muscle bulk, but the inferior division of the oculomotor nerve (n. III) was traced in contiguous image planes to apparently enter the LR muscle. IR: IR muscle; ON: optic nerve; MR: medial rectus muscle; SR: superior rectus muscle. Plane thickness is 2 mm; in-plane resolution is 234 microns.

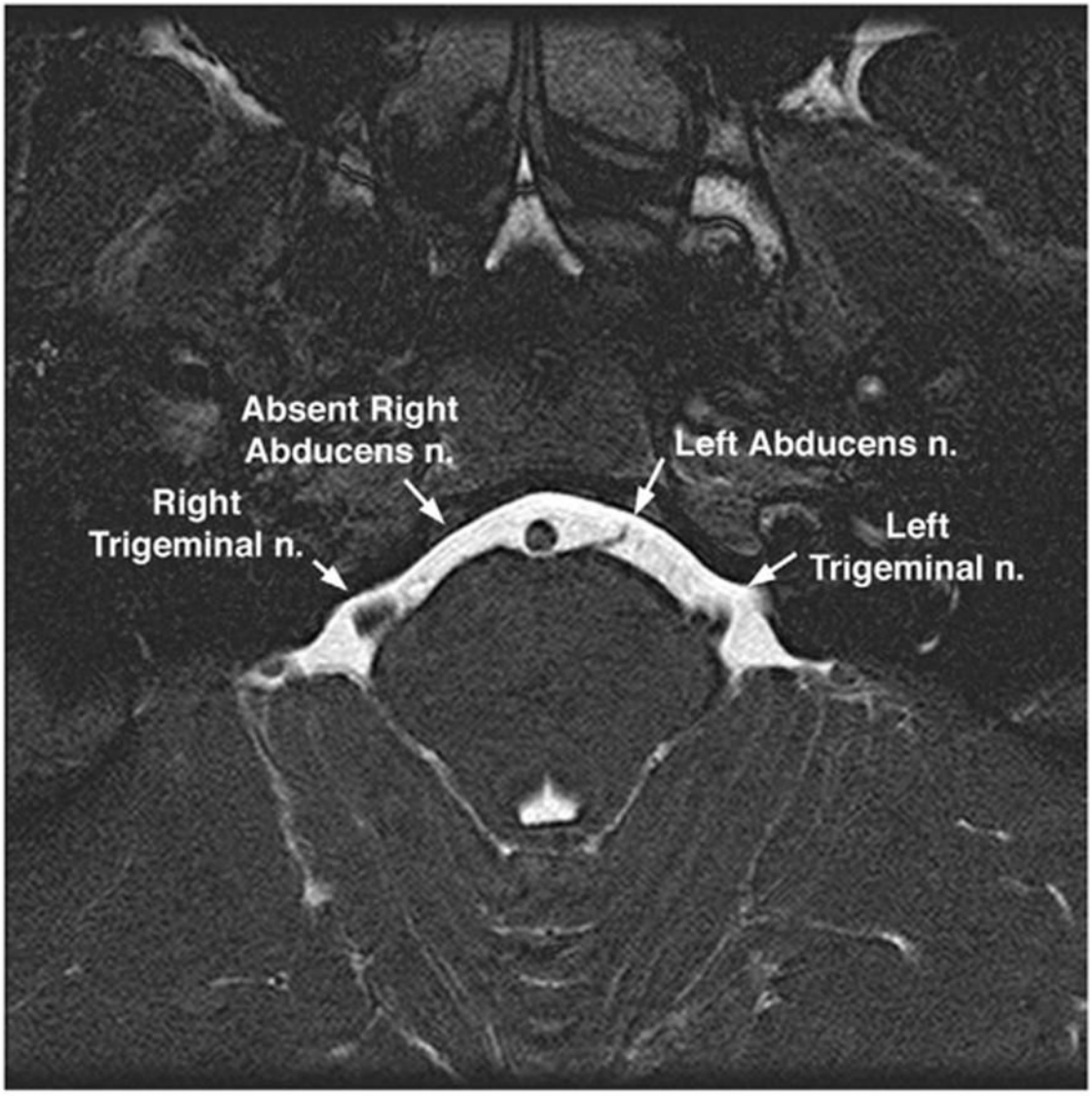


**FIG 12.**

Oblique axial T2-weighted MRI of the midbrain of the patient illustrated in Fig. 11, of a 15-year-old girl with right type 1 Duane syndrome. Note absence of the right abducens nerve, despite presence of the left abducens nerve on the clinically unaffected side. Plane thickness is 1 mm; in-plane resolution is 195 microns.